JOTCS A
Journal of the Turkish Chemical Society
Section: A
Chemistry
TURKISH CHEMICAL SOCIETY

Novel Well-defined Polystyrene-*block*-Poly(lactide-*co*-glycolide) Block Copolymers

Ozcan Altintas*

Department of Chemistry, University of Minnesota, Minneapolis, Minnesota 55455, United States

Abstract: A facile preparation of polystyrene-*block*-poly(lactide-*co*-glycolide) PS-*b*-PLGA block copolymers was reported in detail. Well-defined PS-*b*-PLGA block copolymers were successfully obtained via living anionic polymerization and ring-opening polymerization. First, hydroxyl-terminated linear polystyrenes were prepared by living anionic polymerization. The resulting polymers were used as macroinitiators for ring-opening copolymerization of lactide and glycolide in the presence of the 1,8-diazabicyclo[5.4.0]undec-7-ene (DBU) as a catalyst in dichloromethane at ambient temperature. Transesterification and formation of DBU-initiated polymers were minimized by optimizing the catalyst concentration. Three block copolymers were synthesized in various molecular weights from 5000 g/mol to 33600 g/mol with low polydispersity. The formation of well-defined PS-*b*-PLGA block copolymers was followed by nuclear magnetic resonance spectroscopy and size-exclusion chromatography. Thermal properties of the block copolymers were investigated by thermal gravimetric analysis and differential scanning calorimetry. The morphology of the block copolymers was investigated using small-angle X-ray scattering in the bulk and via grazing incidence small-angle X-ray scattering as well as atomic force microscopy in thin film demonstrating organized nanostructures with uniform domain sizes. Overall, this manuscript describes an expanded polymer toolbox for PLGA-based polymers for next-generation lithography applications.

Keywords: Block copolymers, polystyrene, polyester, morphology, and phase separation.

Submitted: October 12, 2022. **Accepted:** January 09, 2023.

Cite this: Altintas O. Novel Well-defined Polystyrene-block-Poly(lactide-co-glycolide) Block Copolymers. JOTCSA. 2023;10(1):241-52.

DOI: https://doi.org/10.18596/jotcsa.1184492.

***Corresponding author. E-mail:** ozcanaltintas@gmail.com.

1. INTRODUCTION

Block polymers consist of chemically different sub-chains which are covalently attached at junction points (1). Block polymers have gained significant interest in many fields of nanotechnology applications such as fabrication of nanomaterials (2), nanoporous films (3), storage media (4), sensors (5) and nanolithography (6). Block polymers in the bulk or thin film have demonstrated remarkable ability to form well-defined nanostructures because of their microphase separation on the nanoscale (7,8). Block polymer thin films spontaneously produce various well-defined equilibrium morphologies in bulk and solution ranging from spheres, cylinders, lamellae, and more complex structures. The resulting morphologies depend on the following parameters: the number of monomeric units in a block copolymer and the volume fraction of domains as well as the Flory-Huggins parameter (9-11). Lamellae and cylindrical phases are of particular interest in industry (12).

Reversible deactivation radical polymerization (RDRP) techniques (13) such as atom transfer radical polymerization (ATRP) (14,15), reversible addition–fragmentation chain transfer (RAFT) polymerization (16,17) and nitroxide-mediated polymerization (NMP) (18) are the most versatile methods to design and control polymer structure. However, the RDRP methods have their own limitations, including the use of transition metals and sulfur-containing final products as well as slow polymerization rates (19). Among all the living polymerization techniques, anionic polymerization is a unique method for the preparation of polymers with uniform structures (20,21). Well-defined telechelic linear polymers consisting of one or more

functional groups at chain-ends can readily be prepared via living anionic polymerization (21). These functional polymers can be utilized as building blocks such as macroinitiators and cross-linkers for the synthesis of various polymer architectures (22).

Recent years, aliphatic polyesters of lactones and lactides were achieved by ring opening polymerization (ROP) (23-25) have attracted substantial interest due to bacterial decomposition process and forming natural byproducts (26). They have been practiced in various applications ranging from biomedical industries (25) to ordered nanostructured morphologies (19). For example, nanoporous materials can be readily generated from microphase separation of block copolymers having aliphatic polyester and subsequently selective removing of the polyester domains (27,28).

Because of the poor solubility of glycolide and its polymers in common solvents, controlled polymerization of glycolide has been challenging task (29). The copolymerization of lactide and glycolide represents an efficient method to synthesize soluble poly(glycolide) (PGA) derivates. Hoye and coworkers developed a strategy for PLGA-based block copolymers and commercially available hydroxyl functional poly(ethylene glycol) as an initiator using DBU as the catalyst (30). More recently, Long and coworkers synthesized and characterized functional PEG-*b*-PLGA copolymers and studied their subsequent performance in vat photopolymerization for tissue scaffolding applications (31).

To the best of our knowledge, well-defined PS-*b*-PLGA block copolymers via a combination of living anionic polymerization and ROP of lactide and glycolide have not been reported yet. In the current contribution, the goal is to fill this synthetic gap and study the effects of molecular architecture on the resultant thermal and morphlogical properties. First of all, the macroinitiators were prepared by living anionic polymerization using a *sec*-butyl lithium as an intiator. Subsequently, novel PS-*b*-PLGA block copolymers were prepared via ROP of cyclic esters. The resulting block copolymers were characterized via ^{1}H nuclear magnetic resonance (NMR), size exclusion chromatography (SEC), Fourier-transform infrared spectroscopy (FTIR), thermal gravimetric analysis (TGA) and differential scanning calorimetry (DSC). The morphologies of the block copolymers were identified small-angle X-ray scattering (SAXS), atomic force microscopy (AFM) as well as grazing-incidence small-angle scattering (GISAXS).

2. EXPERIMENTAL SECTION

2.1. Materials

Glycolide (99%) and D,L-lactide (99%) were received from Ortec and purified by recrystallization from ethyl acetate and toluene three times, respectively. The monomers were dried in vacuum and brought into the glove box prior to use. DBU (98%), styrene (99%), calcium hydride (CaH_2, 95%), *sec*-butyllithium solution (1.4 M in cyclohexane), di-*n*-butyl magnesium solution (1.0 M in heptane), and ethylene oxide (99.5%) were purchased from Sigma-Aldrich and used as received. Hexafluoro isopropanol (HFIP, 99%) was purchased from Oakwood Chemical and used as received. Methanol, acetone, ethyl acetate, and tetrahydrofuran (THF) were purchased from Sigma-Aldrich as analytical grade and used as received. Solvents for the polymerizations were retrieved from solvent purification columns.

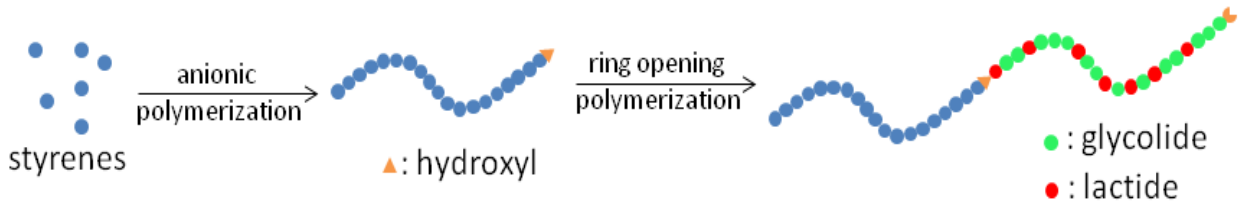

Scheme 1: The preparation of well-defined PS-*b*-PLGA block copolymers.

2.2. Characterization Methods

2.2.1. Nuclear magnetic resonance (NMR) spectroscopy

^{1}H and ^{13}C NMR spectra were obtained using either a 400 or 500 MHz Bruker Avance III HD spectrometer. Chemical shifts were referenced to tetramethylsilane (TMS) as an internal standard at 0.00 ppm for ^{1}H spectra taken in $CDCl_3$ containing 5% w/v TMS.

2.2.2. Size exclusion chromatography (SEC)

SEC ($CHCl_3$ *system*) data was calibrated to polystyrene standards (polymer laboratories) and acquired on a hp 1100 series liquid chromatography with three successive varian plgel mixed-c columns using chloroform as the mobile phase (35 °C, flow rate = 1 mL/min) and an hp 1047a ri detector. SEC (*THF System*) analysis was performed at 25 °C on an Agilent 1260 Infinity liquid chromatography system equipped with three Waters Styragel columns in series, a Wyatt DAWN Heleos II 18-angle light

scattering detector, and a Wyatt OPTILAB T-rEX refractive index detector and using THF as the eluent with a flow rate of 1 mL/min. Polydispersity (*Đ*) was calculated from the light scattering data using Astra software.

2.2.3. Fourier-transform infrared (FT-IR) spectroscopy
Solid-state FT-IR spectra were recorded on a Bruker Alpha Platinum attenuated total reflectance unit (Bruker) coupled to a Bruker Vertex 80 Fourier-transform spectrometer. A series of spectra were collected between 400 and 4000 cm^{-1} in single beam mode using OMNIC software. The measurements were obtained using 164 scans/sample at a resolution of 4 cm^{-1}.

2.2.4. Thermal gravimetric analysis (TGA)
The thermal stability of the polymers was determined using TGA, a TA Instruments Q500. Approximately 5 mg of the polymer was heated at 10 °C/min from ambient temperature to 550 °C in a nitrogen atmosphere.

2.2.5. Differential scanning calorimetry (DSC)
DSC measurements were conducted using a Discovery DSC (TA Instruments Inc.). Approximately 5 mg samples were subjected to a heating and cooling rate of 10 °C/min under nitrogen atmosphere. DSC data analysis was performed using TRIOS software package. The thermal transitions were obtained from the second heating curve. The glass transition temperature (T_g) was determined from the mid-point of the step change in the heat flow signal.

2.2.6. Ellipsometry
The film thicknesses of the freshly spin-coated thin films on the Si wafers were measured by Ellipsometry on a J. A. Wollam Co., Inc. V-VASE.

2.2.7. Atomic force microscopy (AFM)
Tapping mode AFM was performed on a Bruker Nanoscope V Multimode 8 scanning probe microscope under ambient conditions with silicon cantilever tips.

2.2.8. X-ray scattering (SAXS/GISAX)
SAXS experiments at ambient temperature were conducted at the Advanced Photon Source in Argonne National Laboratory (Argonne, IL) using beamline 5-ID-D. SAXS data were collected with an energy 17 keV radiation and a sample-to-detector distance of 6 m. GISAXS measurements were performed at beam line 8-ID-E at the Advanced Photon Source of Argonne National Laboratory. Samples were placed in a vacuum chamber and illuminated with an energy 7.35 keV radiation at incident angles in the range of 0.2-0.24°; the scattering data were recorded with a Pilatus 1MF pixel array detector positioned 2175 mm from the sample. Acquisition times were approximately 10 s per frame.

2.3. Synthesis
2.3.1. Synthesis of ω-(hydroxy)polystyrene homopolymer via anionic polymerization
Following a modified literature procedure (32), hydroxyl functional polystyrenes were synthesized by living anionic polymerization in cyclohexane using sec-butyl lithium as the initiator at 40 °C overnight. Styrene was first freeze-pump-thawed three times and distilled twice over CaH_2 and then once over di-*n*-butylmagnesium and subsequently transferred to a flame-dried air-free burette. Cyclohexane (600 mL) was transferred from the solvent purification columns to a flame-dried air-free flask, then an argon/vacuum manifold, a manometer through Teflon valves, a septum, and the flask of purified styrene (50 g, 0.48 mol) were all connected to a 1-L flask equipped with five internal glass connectors and a Teflon-coated stir bar. The reactor was evacuated with high vacuum of 27 mTorr, flamed-dried and backfilled with argon five times. Finally, the cyclohexane was added to the reactor followed by the addition of *sec*-butyllithium (7.2 mL of 1.40 M *sec*-butyllithium in cyclohexane) with an airtight syringe through the septum. The reaction solution was heated to 40 °C in an oil bath. The styrene was added and the reaction mixture was stirred overnight, observing an orange-red color indicating the presence of poly(styryllithium) chain ends. Ethylene oxide (EO, 5 equivalents to sec-butyllithium initiator) was purified over di-n-butylmagnesium and transferred to a flame-dried air-free burette. The polymerization solution was cooled to the room temperature and the purified ethylene oxide was added by warming small doses from an externally chilled burette connected to the reactor with Ultra-Torr (Swagelok) Cajon tubing. The reaction was allowed to stir overnight under positive pressure. The reaction mixture turned colorless and subsequently was terminated by the addition of degassed methanol. The polymer was isolated by precipitation in cold methanol and the precipitate was filtered off and dried under high vacuum at 70 °C to afford the polymer as a white powder. ^{1}H NMR in $CDCl_3$ {δ, ppm}: 7.40-6.30 (5H, aromatic protons of PS), 3.50-3.20 (2H, CH_2-OH), 1.78-1.18 (aliphatic protons of PS), $M_{n,NMR}$ = 4800 g/mol. $M_{n,SEC}$ = 4900 g/mol, $Đ$ = 1.03.

2.3.2. Synthesis of poly(styrene)-b-poly(glycolide-co-lactide) copolymer via ring opening polymerization
Solutions of the hydroxyl-terminated polystyrene (1 g, 0.208 mmol in 10 mL of DCM), lactide (0.59 g, 4.1 mmol in 18 mL of DCM), 1,8-diazabicyclo[5.4.0] undec-7-ene (DBU, 15 µL in 2 mL of DCM) and glycolide (0.965 g, 8.32 mmol in 20 mL of THF) were first prepared in a controlled atmosphere (nitrogen) glove box. A flame-dried Schlenk flask was then equipped with a septum and a stir bar. The solutions of the macroinitiator and lactide were added to the reaction flask under argon atmosphere, followed by addition of the DBU solution. The solution of glycolide was then added via a syringe pump at a rate of 200 µL/min. At the end of the addition (100 min), solid benzoic acid (25 mg) was added to

terminate the polymerization. The PS-*b*-PLGA block copolymer was purified by precipitation into methanol from the reaction mixture and dried at 60 °C under vacuum overnight. ^{1}H NMR in $CDCl_3$ {δ, ppm}: 7.40-6.30 (5H, aromatic protons of PS), 5.21 (*CH* of PLA), 4.86 (CH_2 of PGA), 1.61 (CH_3 of PLA), 1.78-1.18 (aliphatic protons of PS), $M_{n,NMR}$ = 10800 g/mol, $M_{n,SEC}$ = 9100 g/mol, $Đ$ = 1.15.

3. RESULTS AND DISCUSSIONS

Herein, novel well-defined PS-*b*-PLGA block copolymers were achieved using living anionic polymerization and ROP methods and subsequently morphology of the polymers was investigated in bulk as well as in thin film studies.

Styrene was polymerized using *sec*-BuLi in cyclohexane at 40 °C for 16 hours subsequently ethylene oxide was added to achieve the hydroxyl-terminated polystyrenes. Molecular weight of the homopolymers were determined by ^{1}H NMR and SEC. The SEC traces of the homopolymers demonstrate unimodal molecular weight distributions (refer to Figure S1 in the Supporting Information (SI) section). ^{1}H NMR spectrum (Figure S2 in the SI section) was utilized to estimate the number-average molecular weight, $M_{n,NMR}$, of the homopolymer comparing the integrated areas aromatic protons of the polystyrene at 6.3-7.3 ppm and the nine protons of the initiator at 0.9-1.1 ppm. It was found that molecular weights obtained from both techniques are in excellent agreement. The percentage of the hydroxyl group at chain-end of the homopolymers was estimated by the integral areas of the methylene protons adjacent the hydroxyl group as well as the initiator protons indicating quantitative hydroxyl end-group incorporation (see Table 1).

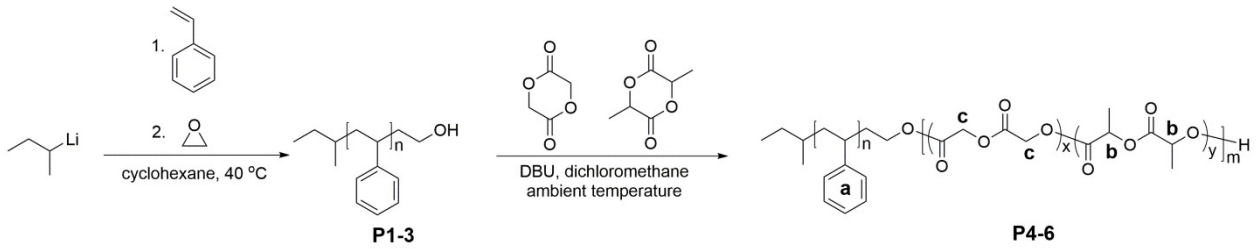

Scheme 2: The chemical structures of the PS-*b*-PLGA block copolymers.

Table 1: Molecular Properties of the PS-OH Macroinitiators.

Polymer	$M_{n,NMR}$[a] (g/mol)	$M_{n,SEC}$[b] (g/mol)	$Đ^b$	EGF[c]
P1	2400	2300	1.03	0.98
P2	4800	4900	1.03	0.99
P3	13700	13400	1.03	0.96

[a]Determined using ^{1}H NMR spectroscopy; [b]determined from SEC in THF using MALLS-SEC; [c]end group fidelity (EGF) or percentage of the hydroxyl group at chain-end.

The ROP of glycolide by Beuermann (29) and lactide by Waymouth (33) has been reported in the absence of any initiator, DBU can act as an initiator to form macrocyclics and linear chains. Thus, the ROP of the cyclic esters was applied both in the presence and absence of a macroinitiator using DBU and observing the formation of oligomeric species in the SEC traces when $[initiator]_0/ [DBU]_0$ = 1 (refer to Figure S3). Subsequently the concentration of DBU was optimized for the ROP of the cyclic esters using the hydroxyl functional polystyrene. After performing the polymerization at various concentration of DBU, it was found that 2 mM concentration of DBU is sufficient to achieve well-defined linear polymers. Next, the block copolymers were accomplished by the ROP of lactide and glycolide using DBU as the catalyst and the hydroxyl-terminated polystyrene as the macroinitiator. The purified block copolymers were characterized by SEC comparing to PS standards using $CHCl_3$ as elution solvent. For example, the SEC trace of P5 in Figure 1 shows a shift towards higher molecular mass, compared with its corresponding polymer precursor (P2). Additionally, no significant increase in the dispersity was observed for the formed block copolymer (PS-*b*-PLGA, P5). Additional details for the macroinitiator and block copolymer are given in Tables 1 and 2. The ^{1}H NMR spectrum of P5 shows corresponding *CH* peak of the PLA and CH_2 of the PGA repeat units at 5.21 ppm and 4.86 ppm, respectively, confirming successful block copolymer incorporation (refer to Figure 2). The $M_{n,NMR}$ of the block copolymers was obtained by using the aromatic protons of PS, the CH of the PLA and the two protons of PGA. Volume fractions of PLA and PGA segments in the block copolymer were

calculated using ^{1}H NMR spectrum based on homopolymer densities. In addition, the lactide/glycolide weight fractions of the block copolymers were obtained from integral area of the peaks at 5.21 ppm and 4.86 ppm, respectively and reported in Table 2. Further evidence for the block copolymer formation was obtained from FT-IR (refer to Figure S4) as the carbonyl stretching band of the PLGA chains were appeared at 1754 cm^{-1}.

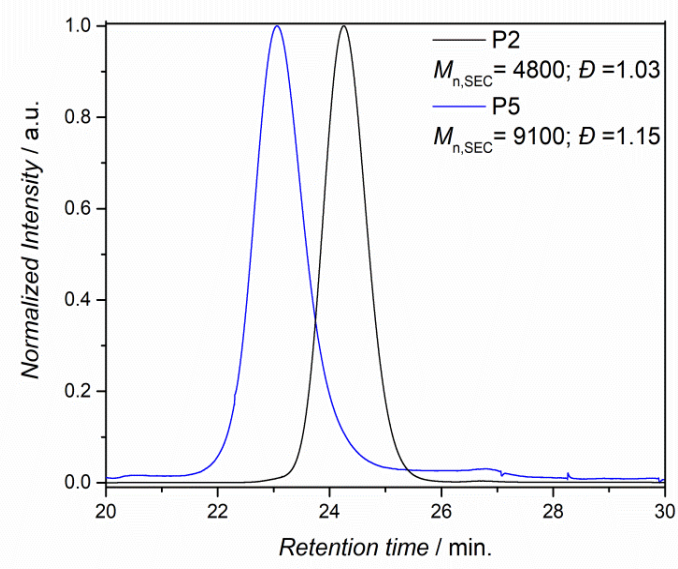

Figure 1: SEC traces of the hydroxyl-terminated polystyrene (P2) and the corresponding block copolymer (PS-*b*-PLGA, P5). Additional details for the macroinitiator and block copolymers are given in Tables 1 and 2 as well as Figure S1 and S2.

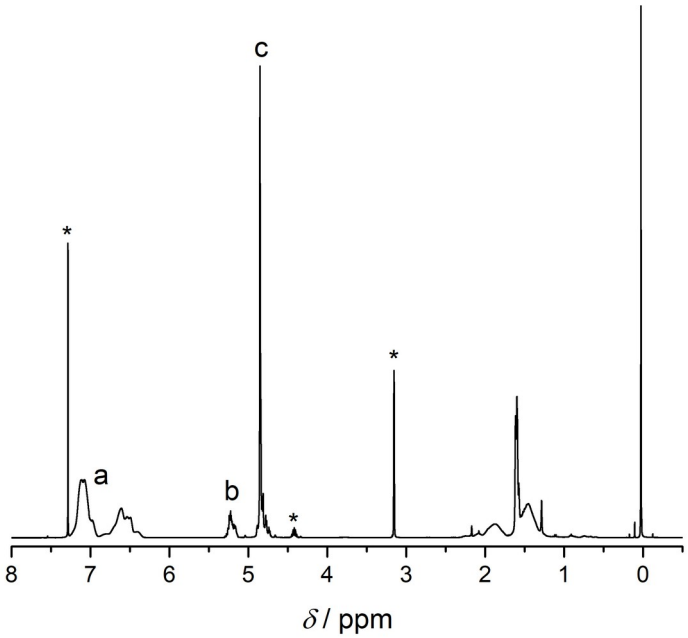

Figure 2: ^{1}H NMR spectra of PS-*b*-PLGA (P5) in $CDCl_3$/hexafluoro-2-propanol (HFIP) (v/v: 9/1) at ambient temperature. The peaks marked with an asterisk are due to solvent (HFIP). The chemical structures can be found in Scheme 2.

The thermal behavior of the PS-*b*-PLGA block copolymers was examined via TGA heating from room temperature to 550 °C at a rate of 10 °C/min under nitrogen which are depicted in Figure 3. The PS-*b*-PLGA block copolymers demonstrated a two-step weight loss. Initially the block copolymers lost ~60% weight at 350 °C corresponding to the PLGA thermal degradation temperature and subsequently complete degradation occurred at 420 °C referring to the decomposition of PS.

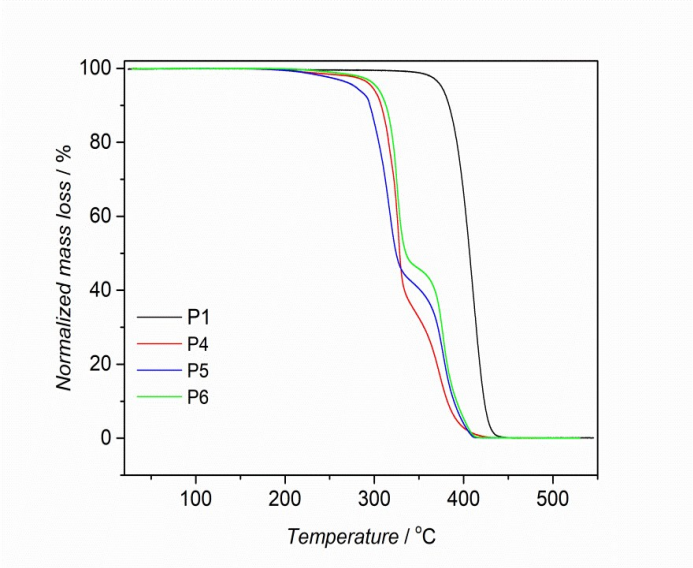

Figure 3: TGA traces of block copolymers and precursor polymer.

The thermal transitions of the block copolymer were investigated using DSC in order to observe the glass transition temperatures (T_g) and the peak melting temperature (T_m). The second heating traces of the block copolymers are shown in Figure 4. The DSC trace of the PS-*b*-PLGA block copolymer (P6) shows a T_g at 43 °C corresponding to the PLGA chains, then a second glass transition at about 96 °C referring to the T_g of the PS chains, which are in excellent agreement with reported values (29). Upon further heating, melting of the semi-crystalline domains of PLGA is detected by observing the T_m at ~150 °C. The degree of crystallinity (X_c) of PS-*b*-PLGA block copolymers was calculated by the following literature (32).

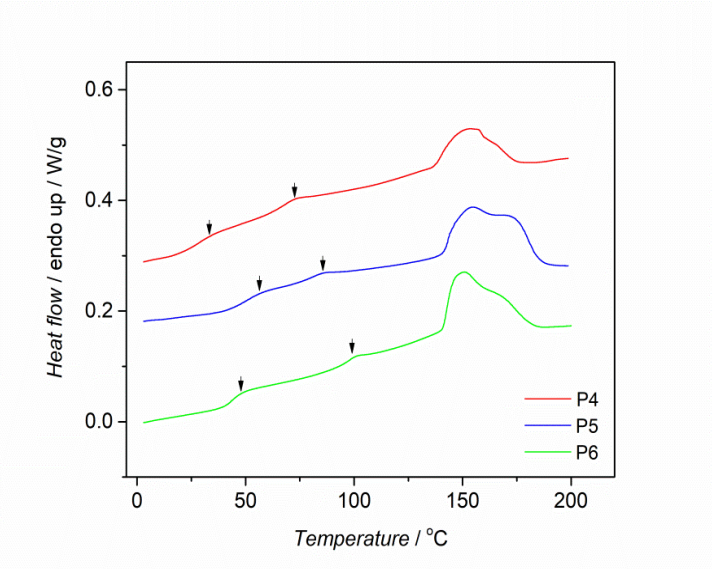

Figure 4: DSC traces for PS-*b*-PLGA block copolymers.

Table 2: Molecular and Thermal Characteristics of Block Copolymers.

Polymer	$M_{n,NMR}$[a] (g/mol)	$M_{n,SEC}$[b] (g/mol)	$Đ$[b]	f_{PLGA}[c]	w_{PGA}[d]	$T_{g,PS}$[e] (°C)	$T_{g,PLGA}$[f] (°C)	$T_{m,PGA}$[g] (°C)	X_c[h] (%)	T_d[i] (°C)	D_{SAXS}[k] (nm)
P4	5000	5500	1.16	0.45	0.33	68	26	166	30	298	15
P5	10800	9100	1.15	0.48	0.38	83	49	169	25	285	16
P6	33600	19500	1.17	0.52	0.31	98	43	147	29	308	27

[a]Calculated using ^{1}H NMR spectra. [b]Determined via SEC. [c]Volume fraction of PLGA. [d]Weight fraction of PLGA. [e]$T_{g,PS}$ is the glass transition temperature of the PS and [f]$T_{g,PLGA}$ is for the PLGA. [g]$T_{m,PGA}$ is PLGA melting temperature. [h]Degree of crystallinity. [i]5% mass loss was determined by TGA. [k]Domain spacing was obtained from SAXS data.

The morphology of the block copolymers was investigated via SAXS. The block copolymers were annealed at 110 °C under inert atmosphere for 16 h. Subsequently the block copolymers were slowly cooled to the room temperature before examining the bulk microphase separation via SAXS. Domain spacings ($D = 2\pi/q^*$) were obtained by using the principal scattering peak position (q^*) and summarized in Table 2. The SAXS scattering profiles of the block copolymers at 25 °C show a main scattering peak with domain spacing of 15-27 nm, which indicates microphase separation. Because of the lack of well-defined second order reflections, the morphology of the block copolymers could not be determined via SAXS (Figure 5). It is possible that the polymer chains were not able to move in bulk below the melting temperature due to their semi-crystalline nature.

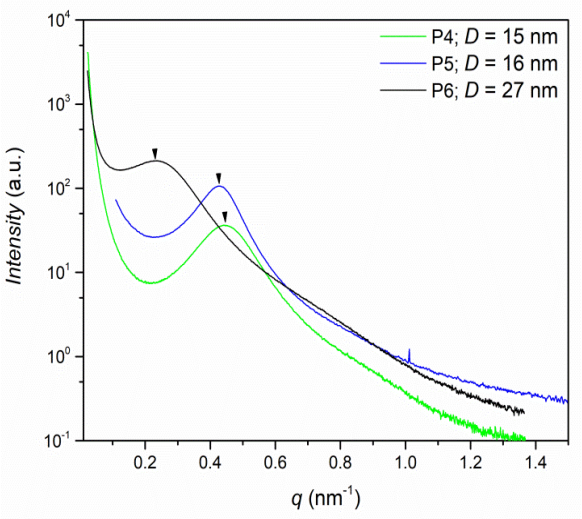

Figure 5: The SAXS data obtained at ambient temperature for the corresponding block copolymers.

Subsequently the surface phase structures of polymer films were analyzed by AFM (35). Block copolymer solutions (10 mg/mL) in $CHCl_3$/HFIP (v/v: 9/1) were spin-coated onto HMDS-modified silicon wafers. The thickness of the polymer film, measured by ellipsometer, was around 54 nm. Solvent vapor annealed (SVA) was applied in $CHCl_3$/HFIP (v/v: 9/1) for five minutes (36). After SVA, the thin film was analyzed by AFM in the tapping mode showing the image in Figure 6. The AFM characterization of P5 demonstrated well-segregated microdomains with uniform domain size throughout the 1 x 1 µm sample suggesting possible perpendicular lamellar orientation in the PS-*b*-PLGA thin films (Figure 5). The domain spacing from the AFM image (20 nm) and SAXS (16 nm) is comparable.

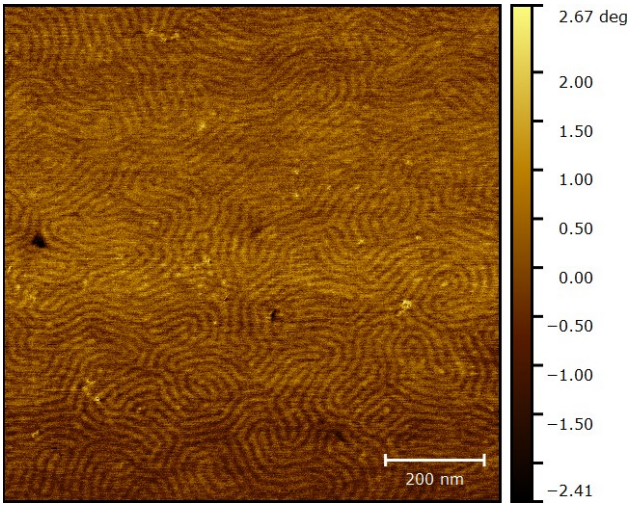

Figure 6: AFM phase image of PS-*b*-PLGA (P5).

The morphological characterization in block polymer thin films can be obtained through the small-angle X-ray scattering (GISAXS) technique (37). In addition to SAXS and AFM characterizations, the one-

dimensional GISAX data for P5 was shown in Figure 7. The fundamental domain spacing was estimated to be 15.8 nm from the principle scattering peak maxima at q_y^* = 0.396/nm. Because of the symmetric volume fractions of each segment (f_{PLGA} = 0.48), it might be indicative of a lamellar morphology (38). Moreover, the spacing of the features from the GISAXS (15.8 nm) is in excellent agreement with the bulk spacing obtained by SAXS (16 nm). Based on the DSC, AFM and GISAXS analysis, the symmetric PS-*b*-PLGA block copolymer could be microphase-separated with a perpendicular lamellar morphology.

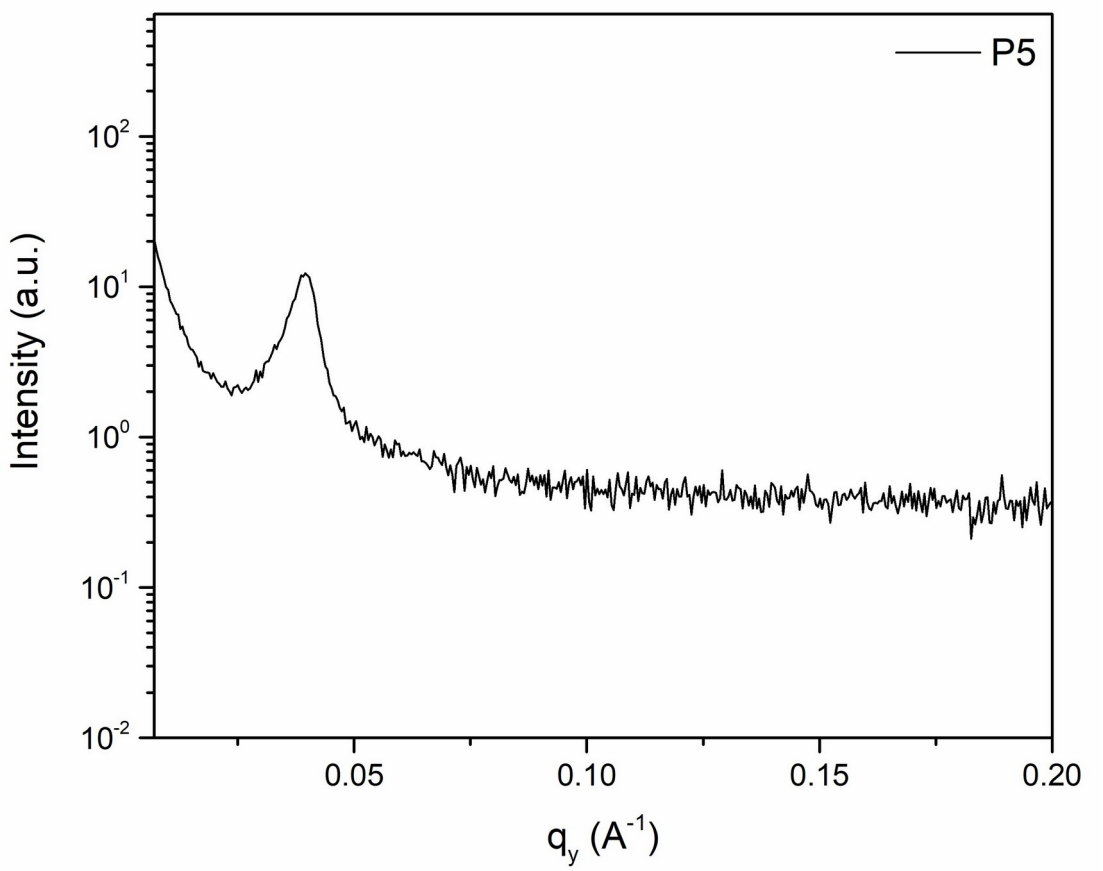

Figure 7: 1D synchrotron GISAXS profile for the block copolymer (P5, $M_{n,NMR}$ = 10800 g/mol, f_{PLGA} = 0.48) at room temperature.

4. CONCLUSION

A versatile synthetic approach for the synthesis of PS-*b*-PLGA block copolymers was -for the first time- demonstrated. Well-defined PS-*b*-PLGA polymers were successfully obtained via advanced polymerization methods. Initially hydroxyl-terminated linear polystyrenes were prepared and then copolymerization of lactide and glycolide was achieved using the macroinitiator and DBU at ambient temperature leading to PS-*b*-PLGA block copolymers. Transesterification and formation of DBU-initiated polymers were minimized by optimizing the catalyst concentration to 2 mM. Number-average molar mass of the block copolymers as well as the block volume fraction were calculated based on ^{1}H NMR spectra. Furthermore, the block copolymer formation was followed by SEC traces. The stability of the block copolymer was analyzed by TGA demonstrating less than 5% weight loss up to 270 °C. Thermal properties of the block copolymer were obtained by DSC indicating two clear glass transition and melting temperatures suggesting well-defined microphase separation. The formation of the organized nanostructures was observed by SAXS, GISAXS and AFM. Although no higher order reflections were observed in the SAXS characterization, these polymers have a fundamental spacing ranging of 15-27 nm. The results from DSC, AFM and GISAXS demonstrate that the morphology of the block copolymer is presumably perpendicular lamellar as each segment (f_{PLGA} = 0.48) has the symmetric volume fractions. The present results unambiguously prove that the formation of PS-*b*-PLGA block copolymers on a very well-defined level is indeed possible employing high precision macromolecular design strategies. This manuscript have demonstrated the synthesis, characterization, and morphology of PLGA-based block copolymers as well as potential use in nanopatterning and advanced multilayer applications.

5. ACKNOWLEDGMENTS

The author graciously thanks Prof. Marc Hillmyer (UMN), Prof. Frank Bates (UMN), and Dr. Joshua Speros (BASF) for helpful discussion as well as for their financial support. SAXS and GISAXS data were obtained at the Advanced Photon Source, a U.S. Department of Energy (DOE) Office of Science User Facility operated for the DOE Office of Science by Argonne National Laboratory. Parts of this work were carried out in the Characterization Facility, University of Minnesota.

6. REFERENCES

1. Bates CM, Bates FS. 50th Anniversary Perspective : Block Polymers—Pure Potential. Macromolecules. 2017 Jan 10;50(1):3–22. Available from: <URL>.

2. Lazzari M, López-Quintela MA. Block Copolymers as a Tool for Nanomaterial Fabrication. Adv Mater. 2003 Oct 2;15(19):1583–94. Available from: <URL>.

3. Jackson EA, Hillmyer MA. Nanoporous Membranes Derived from Block Copolymers: From Drug Delivery to Water Filtration. ACS Nano. 2010 Jul 27;4(7):3548–53. Available from: <URL>.

4. Kim HC, Park SM, Hinsberg WD. Block Copolymer Based Nanostructures: Materials, Processes, and Applications to Electronics. Chem Rev. 2010 Jan 13;110(1):146–77. Available from: <URL>.

5. Jung YS, Jung W, Tuller HL, Ross CA. Nanowire Conductive Polymer Gas Sensor Patterned Using Self-Assembled Block Copolymer Lithography. Nano Lett. 2008 Nov 12;8(11):3776–80. Available from: <URL>.

6. Park M, Harrison C, Chaikin P, others. Block Copolymer Lithography: Periodic Arrays of 10. Holes in. 1:1401–4.

7. Bates FS, Hillmyer MA, Lodge TP, Bates CM, Delaney KT, Fredrickson GH. Multiblock Polymers: Panacea or Pandora's Box? Science. 2012 Apr 27;336(6080):434–40. Available from: <URL>.

8. Darling SB. Directing the self-assembly of block copolymers. Progress in Polymer Science. 2007 Oct;32(10):1152–204. Available from: <URL>.

9. Leibler L. Theory of microphase separation in block copolymers. Macromolecules. 1980;13(6):1602–17.

10. Bates FS. Polymer-Polymer Phase Behavior. Science. 1991 Feb 22;251(4996):898–905. Available from: <URL>.

11. Bates FS, Fredrickson GH. Block copolymers-designer soft materials. Physics today. 2000;52.

12. Luo M, Epps TH. Directed Block Copolymer Thin Film Self-Assembly: Emerging Trends in Nanopattern Fabrication. Macromolecules. 2013 Oct 8;46(19):7567–79. Available from: <URL>.

13. Klumperman B. Reversible Deactivation Radical Polymerization. In: John Wiley & Sons, Inc., editor. Encyclopedia of Polymer Science and Technology [Internet]. 1st ed. Wiley; 2015 [cited 2023 Feb 8]. p. 1–27. Available from: <URL>.

14. Matyjaszewski K. Atom Transfer Radical Polymerization (ATRP): Current Status and Future Perspectives. Macromolecules. 2012 May 22;45(10):4015–39. Available from: <URL>.

15. Ouchi M, Sawamoto M. 50th Anniversary Perspective : Metal-Catalyzed Living Radical Polymerization: Discovery and Perspective. Macromolecules. 2017 Apr 11;50(7):2603–14. Available from: <URL>.

16. Perrier S. 50th Anniversary Perspective : RAFT Polymerization—A User Guide. Macromolecules. 2017 Oct 10;50(19):7433–47. Available from: <URL>.

17. Moad G. RAFT polymerization to form stimuli-responsive polymers. Polym Chem. 2017;8(1):177–219. Available from: <URL>.

18. Nicolas J, Guillaneuf Y, Lefay C, Bertin D, Gigmes D, Charleux B. Nitroxide-mediated polymerization. Progress in Polymer Science. 2013 Jan;38(1):63–235. Available from: <URL>.

19. Vanderlaan ME, Hillmyer MA. "Uncontrolled" Preparation of Disperse Poly(lactide)- block -poly(styrene)-block -poly(lactide) for Nanopatterning Applications. Macromolecules. 2016 Nov 8;49(21):8031–40. Available from: <URL>.

20. Szwarc M. 'Living'polymers. Nature. 1956;178:1168–9.

21. Hirao A, Loykulnant S, Ishizone T. Recent advance in living anionic polymerization of functionalized styrene derivatives. Progress in Polymer Science. 2002 Oct;27(8):1399–471. Available from: <URL>.

22. Hadjichristidis N, Pitsikalis M, Pispas S, Iatrou H. Polymers with Complex Architecture by Living Anionic Polymerization. Chem Rev. 2001 Dec 1;101(12):3747–92. Available from: <URL>.

23. Dechy-Cabaret O, Martin-Vaca B, Bourissou D. Controlled Ring-Opening Polymerization of Lactide and Glycolide. Chem Rev. 2004 Dec 1;104(12):6147–76. Available from: <URL>.

24. Meduri A, Fuoco T, Lamberti M, Pellecchia C, Pappalardo D. Versatile Copolymerization of Glycolide and rac -Lactide by Dimethyl(salicylaldiminato)aluminum Compounds. Macromolecules. 2014 Jan 28;47(2):534–43. Available from: <URL>.

25. Albertsson AC, Varma IK. Recent Developments in Ring Opening Polymerization of Lactones for Biomedical Applications. Biomacromolecules. 2003 Nov 1;4(6):1466–86. Available from: <URL>.

26. Chiellini E, Solaro R. Biodegradable Polymeric Materials. Adv Mater. 1996 Apr;8(4):305–13. Available from: <URL>.

27. Saba SA, Mousavi MPS, Bühlmann P, Hillmyer MA. Hierarchically Porous Polymer Monoliths by Combining Controlled Macro- and Microphase Separation. J Am Chem Soc. 2015 Jul 22;137(28):8896–9. Available from: <URL>.

28. Altay E, Jang YJ, Kua XQ, Hillmyer MA. Synthesis, Microstructure, and Properties of High-Molar-Mass Polyglycolide Copolymers with Isolated Methyl Defects. Biomacromolecules. 2021 Jun 14;22(6):2532–43. Available from: <URL>.

29. Kemo VM, Schmidt C, Zhang Y, Beuermann S. Low Temperature Ring-Opening Polymerization of Diglycolide Using Organocatalysts with PEG as Macroinitiator. Macromol Chem Phys. 2016 Apr;217(7):842–9. Available from: <URL>.

30. Qian H, Wohl AR, Crow JT, Macosko CW, Hoye TR. A Strategy for Control of "Random" Copolymerization of Lactide and Glycolide: Application to Synthesis of PEG- b -PLGA Block Polymers Having Narrow Dispersity. Macromolecules. 2011 Sep 27;44(18):7132–40. Available from: <URL>.

31. Wilts EM, Gula A, Davis C, Chartrain N, Williams CB, Long TE. Vat photopolymerization of liquid, biodegradable PLGA-based oligomers as tissue scaffolds. European Polymer Journal. 2020 May;130:109693. Available from: <URL>.

32. Zalusky AS, Olayo-Valles R, Wolf JH, Hillmyer MA. Ordered Nanoporous Polymers from Polystyrene−Polylactide Block Copolymers. J Am Chem Soc. 2002 Oct 1;124(43):12761–73. Available from: <URL>.

33. Brown HA, De Crisci AG, Hedrick JL, Waymouth RM. Amidine-Mediated Zwitterionic Polymerization of Lactide. ACS Macro Lett. 2012 Sep 18;1(9):1113–5. Available from: <URL>.

34. Chu CC. Differential scanning calorimetric study of the crystallization kinetics of polyglycolic acid at high undercooling. Polymer. 1980 Dec;21(12):1480–2. Available from: <URL>.

35. Wang D, Russell TP. Advances in Atomic Force Microscopy for Probing Polymer Structure and Properties. Macromolecules. 2018 Jan 9;51(1):3–24. Available from: <URL>.

36. Yao L, Oquendo LE, Schulze MW, Lewis RM, Gladfelter WL, Hillmyer MA. Poly(cyclohexylethylene)- block -Poly(lactide) Oligomers for Ultrasmall Nanopatterning Using Atomic Layer Deposition. ACS Appl Mater Interfaces. 2016 Mar 23;8(11):7431–9. Available from: <URL>.

37. Posselt D, Zhang J, Smilgies DM, Berezkin AV, Potemkin II, Papadakis CM. Restructuring in block copolymer thin films: In situ GISAXS investigations during solvent vapor annealing. Progress in Polymer Science. 2017 Mar;66:80–115. Available from: <URL>.

38. Vora A, Wojtecki RJ, Schmidt K, Chunder A, Cheng JY, Nelson A, et al. Development of polycarbonate-containing block copolymers for thin film self-assembly applications. Polym Chem. 2016;7(4):940–50. Available from: <URL>.

Novel Well-defined Polystyrene-*block*-Poly(lactide-*co*-glycolide) Block Copolymers

SUPPORTING INFORMATION

Ozcan Altintas*

Department of Chemistry, University of Minnesota, Minneapolis, Minnesota 55455, United States

*Corresponding author (e-mail: ozcanaltintas@gmail.com)

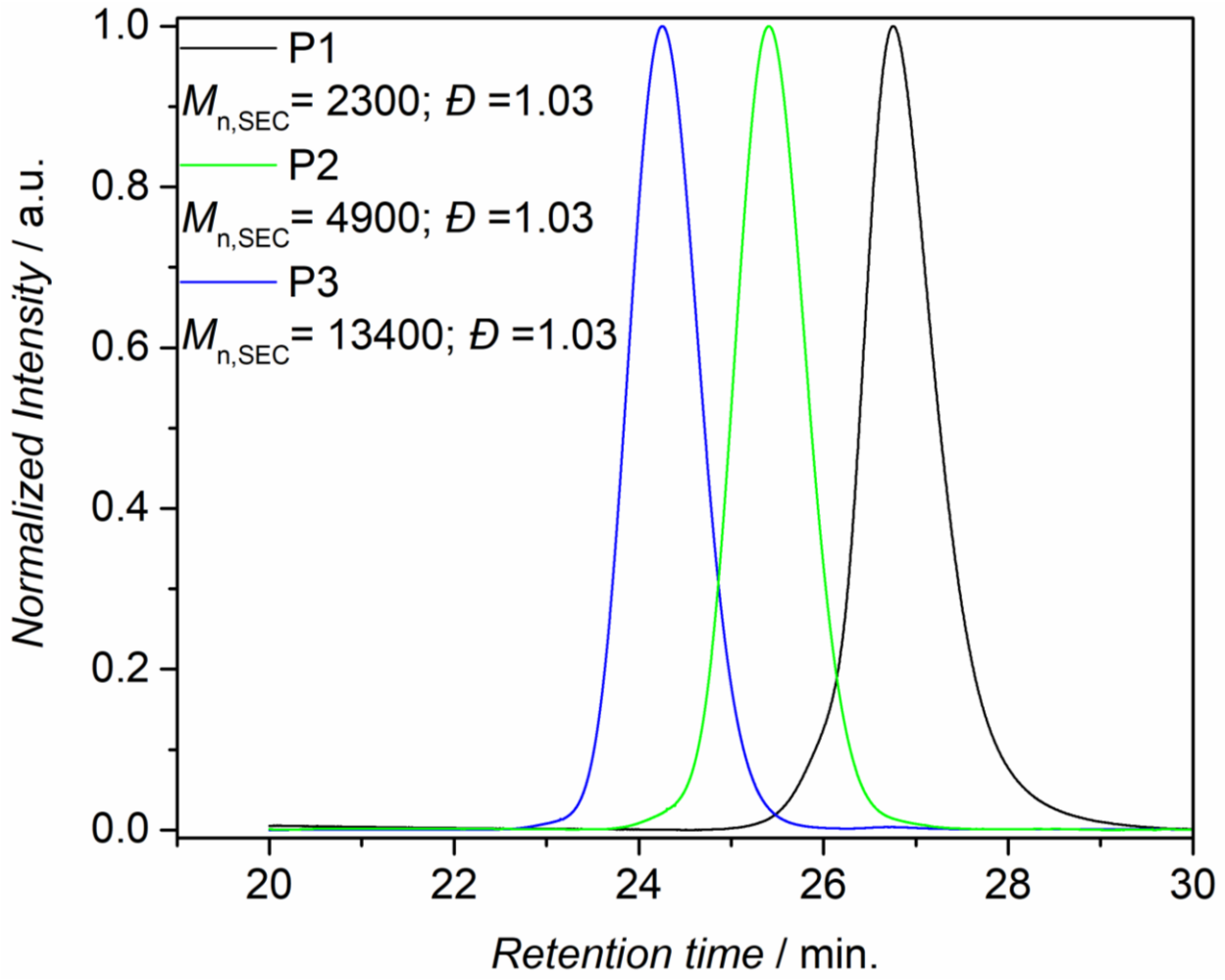

Figure S1. SEC traces of the precursor polymers (P1, P2, P3) using THF as the eluent.

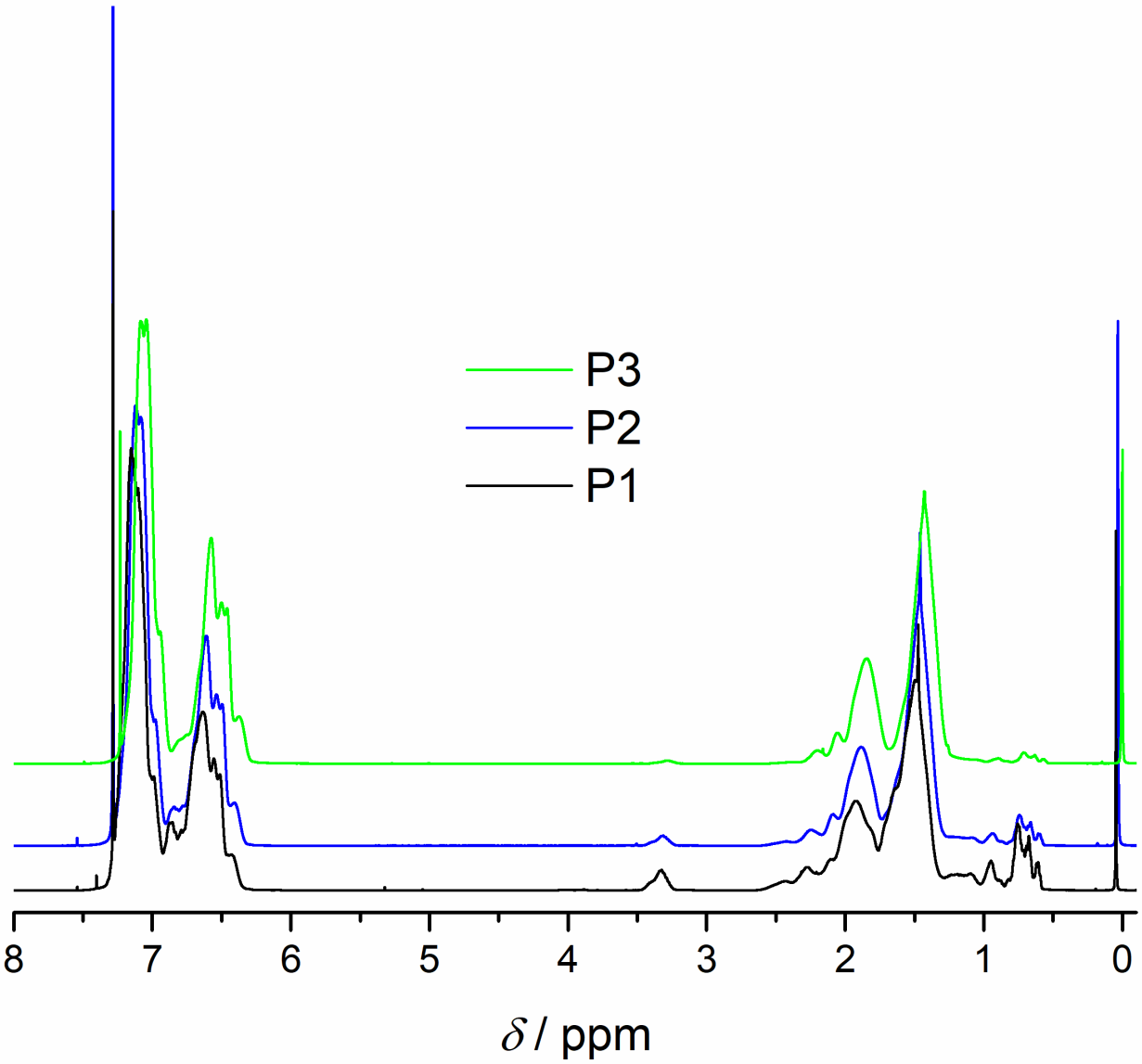

Figure S2. ^{1}H NMR spectra of the precursor polymers (**P1**, **P2**, **P3**) in $CDCl_3$ at the ambient temperature.

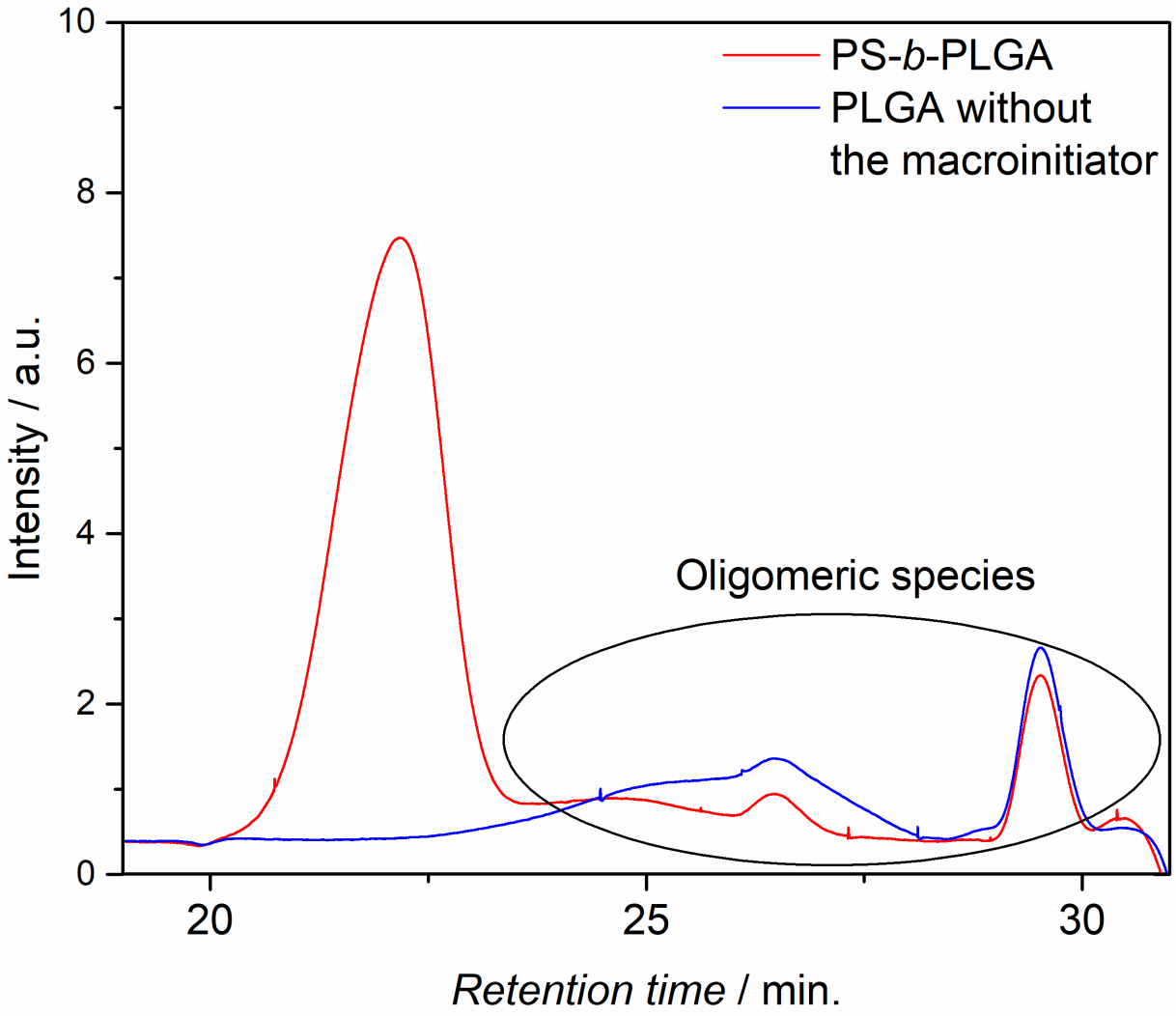

Figure S3. SEC traces of the test polymerizations using $CHCl_3$ as the eluent and calibrated vs. polystyrene standards.

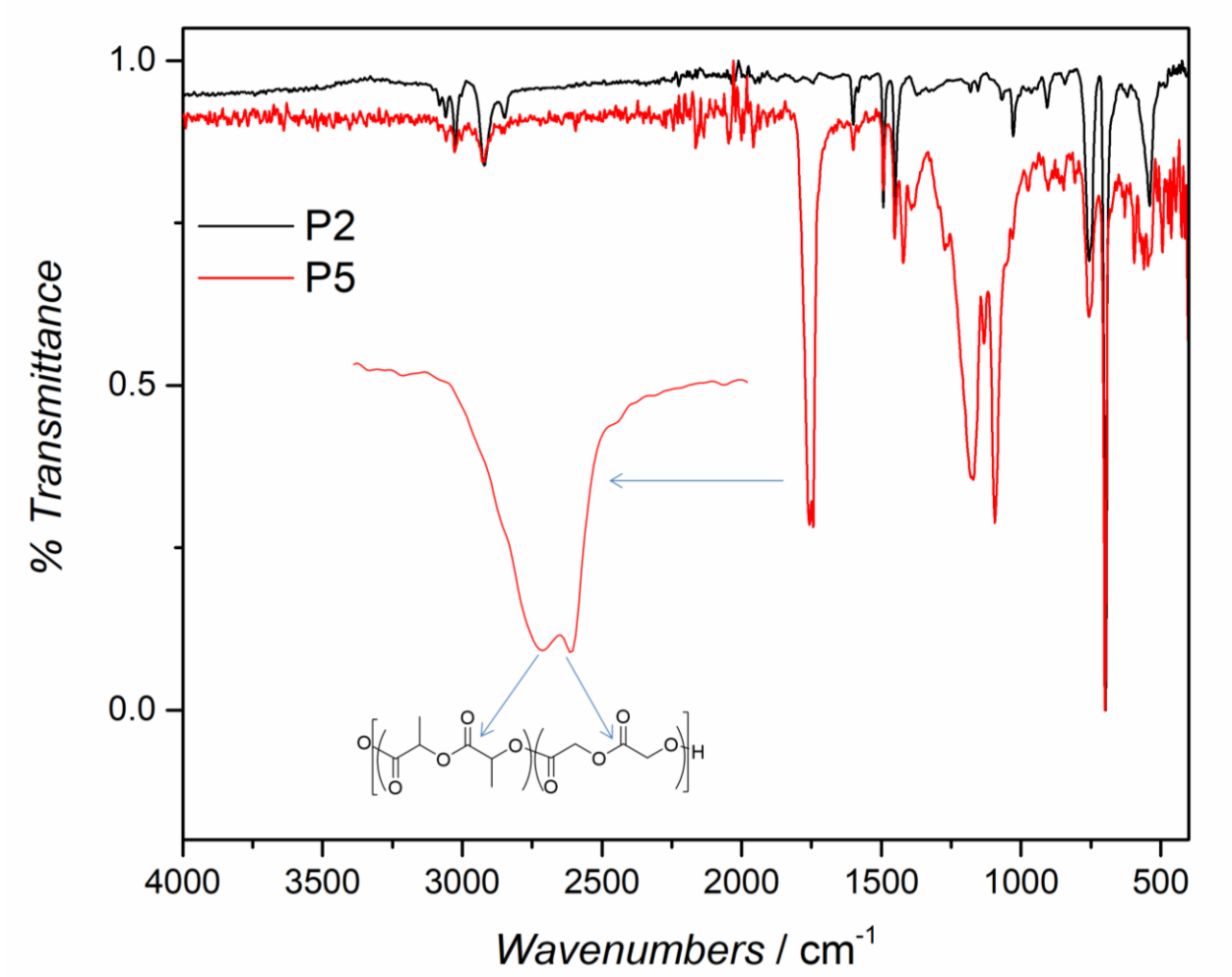

Figure S4. FT-IR spectra of the precursor polymer and corresponding block polymer.

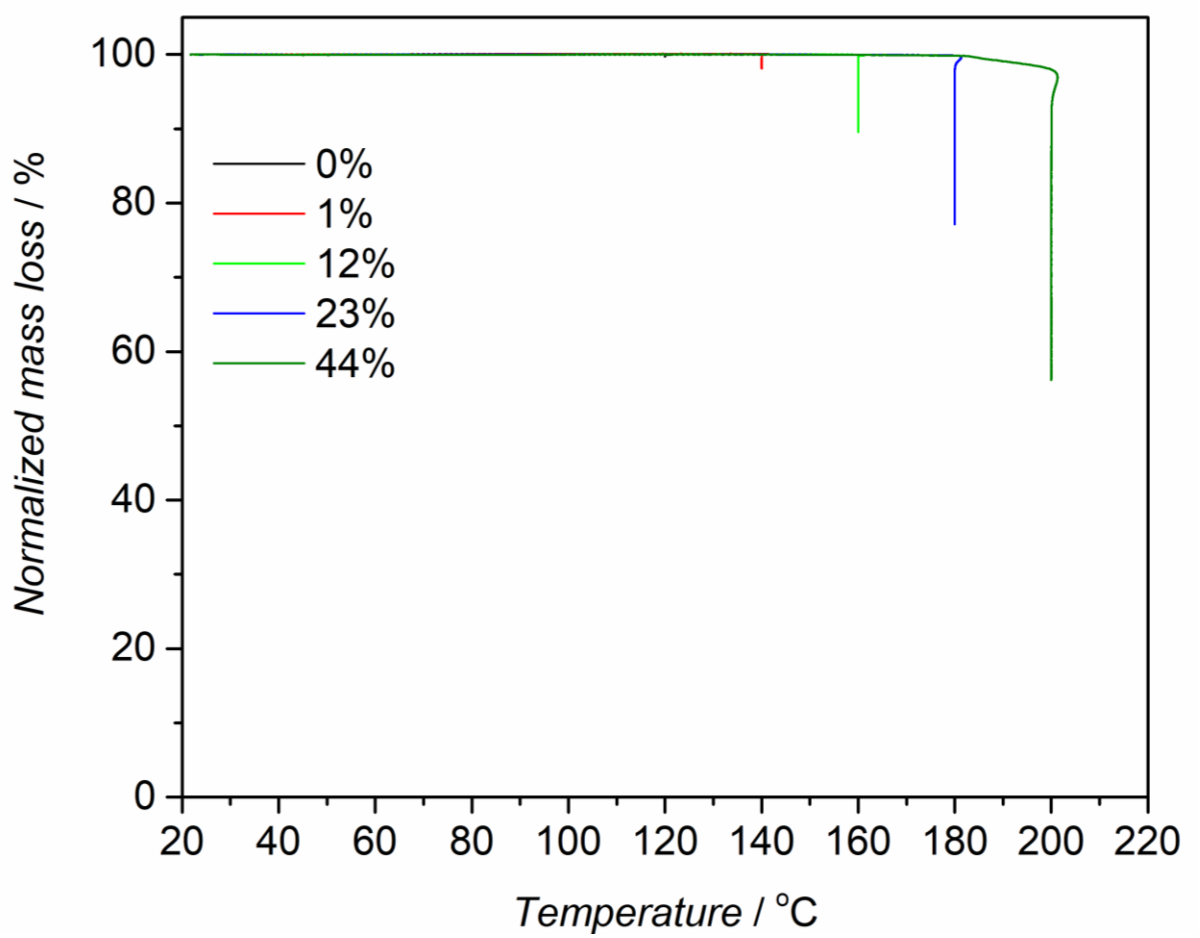

Figure S5. TGA traces of block copolymers at various temperatures for 3 hours with a heating rate of 10°C·min^{-1} under nitrogen atmosphere.

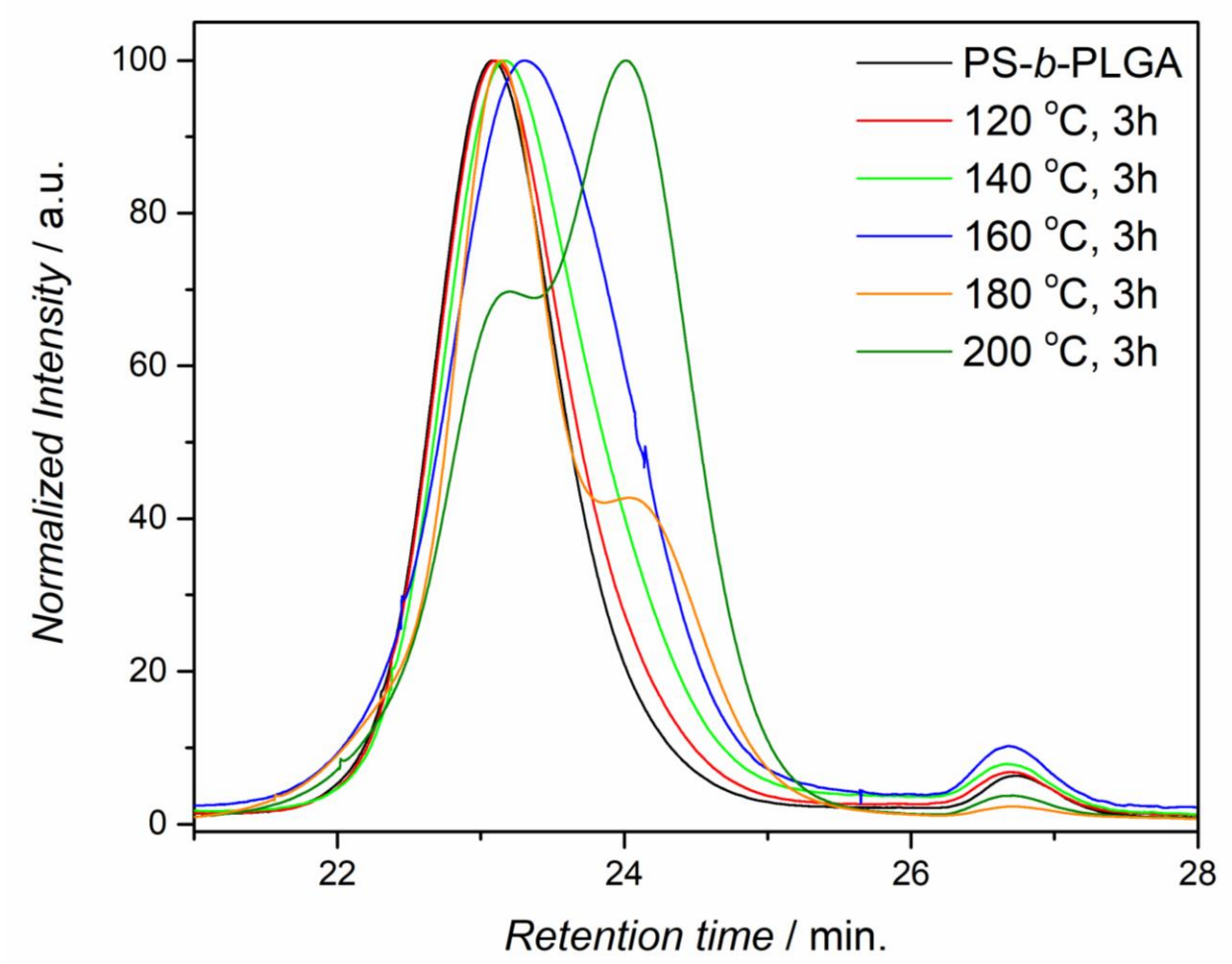

Figure S6. Evolution of the molecular weight distribution of the block polymer (P3) at various temperatures for 3 h under inert atmosphere.